Afyon Kocatepe Üniversitesi Fen ve Mühendislik Bilimleri Dergisi

Afyon Kocatepe University Journal of Science and Engineering

AKÜ FEMÜBİD **21** (2021) 025203 (326-336) AKU J. Sci. Eng. **21** (2021) 025203 (326-336)

DOI: 10.35414/akufemubid.889877

Araştırma Makalesi / Research Article

BLDC Motor Design and Application for Light Electric Vehicle

Mehmet AKAR[1], Mustafa EKER[2*], Fazilet AKIN[3]

[1,2,3] *Department of Mechatronics Engineering, Faculty of Engineering and Architecture Sciences, Gaziosmanpasa University, Tokat, 60150, Turkey*

Sorumlu yazar e-mail: mustafa.eker@gop.edu.tr ORCID ID: https://orcid.org/0000-0003-1085-0968

mehmet.akar@gop.edu.tr. ORCID ID: https://orcid.org/0000-0003-0164-1451

fazilet.akin9358@gmail.com ORCİD ID: *https://orcid.org/0000-0002-8882-2695*

Geliş Tarihi: 03.03.2021 Kabul Tarihi: 13.04.2021

Keywords
BLDC; Electrical Vehicle; Finite Elements Method; Efficiency

Abstract

The popularity of electrical vehicles is increasing rapidly in recent years due to energy generation/consumption ratio, transportation costs, decrease in fossil fuel reserves with increasing population as well as the environmental damage caused by fossil fuels. Therefore, Brushless Direct Current (BLDC) Motor design was actualized in the present study for use in electrical vehicles expected to replace the transportation vehicles of today. Firstly, analytical design of the targeted motor was completed after which the Finite Elements Method was used for modelling. Ansys Maxwell Program is one of the package programs used in FEM. This study was carried out with Ansys Maxwell Electromagnetic Suite version 17.2 . The prototype motor was manufactured after reaching the desired results with Finite Elements Method and experimental studies commenced with the experiment setup prepared in the laboratory environment. Experimental results were compared with electromagnetic results. Finally, the prototype motor was mounted on the ElektroGOP vehicle and it was observed to work without problem at the expected performance during the test drives.

Hafif Elektrikli Araç için FDAM Tasarım ve Uygulaması

Anahtar Kelimeler
FDAM; Elektrikli Araçlar; Sonlu Elemanlar Yöntemi; Verimlilik

Öz

Son yıllarda artan nüfusla birlikte enerji üretim/tüketim oranı, ulaşım giderleri, fosil yakıt rezervlerinin azalması ve fosil yakıtların çevreye verdikleri zararlar gibi başlıca etkenler sebebiyle elektrikli araçların popülaritesi hızlı bir şekilde artmaktadır. Dolasıyla elektrikli araç ve ekipmanları üzerine yapılan çalışmalar da artmaktadır. Bu çalışmada günümüz ulaşım araçlarının yerini alan elektrikli araçlarda kullanılması hedeflenen Fırçasız Doğru Akım Motor (FDAM) tasarımı gerçekleştirilmiştir. Öncelikle hedeflenen motorun analitik tasarımı yapılarak Sonlu Elemanlar Yöntemi (SEY) ile modellemesi yapılmıştır. Ansys Maxwell Programı SEY'de kullanılan paket programlardan biridir. Bu çalışma Ansys Maxwell Elektromanyetik Suite 17.2 versiyonu ile gerçekleştirilmiştir. SEY ile hedeflenen sonuçlara ulaşıldıktan sonra motorun protorip üretimi gerçekleştirilmiş ve prototip motorun, laboratuvar ortamında hazırlanan deney düzeneği ile deneysel çalışmaları yapılmıştır. Deneysel sonuçlar elektromanyetik sonuçlarla karşılaştırılmıştır. Son olarak prototip motor ElektroGOP aracına monte edilmiş ve sürüş denemelerinde motorun hedeflenen performansta ve sorunsuz şekilde çalıştığı görülmüştür.

1. Introduction

Transportation is one of our fundamental needs since ancient times. Fossil fuel based transportation vehicles hold an important place in today's vehicle technology. The reserve issues and adverse environmental impacts of fossil fuels is a well-known fact by everyone. Hence, researches/studies for using different propulsion systems in transportation vehicles continue to increase rapidly in recent years (Hori 2004, Uçarol 2003). It is predicted that Electrical Vehicles (EV) will be preferred more in the future for reducing fossil fuel related air pollution, worldwide greenhouse gases and fossil based fuels along with transportation

costs (Tur *et al*. 2005). The minimum level of environmental damage caused by EVs supports this prediction.

The idea of EV first emerged during the 19th century and studies have been ongoing until today. It has now become possible to see electrical, light electrical and hybrid vehicles with EV technology up and running on the roads (Ustun *et al*. 2009, Tutelea and I. Boldea 2007, Zarko *et al*. 2007). The first industrial applications were carried out by Ford (1967) and General Electric (1967) (Gökce 2005, Uçarol 2003). While DC propulsion was used in the first vehicles together with lead-acid type batteries, different battery types have started to be used together with the implementation of AC propulsion (Tur 2007). Semi-conductor technology and new control methods were developed and improved during the 1990's. Moreover, DC systems started to be replaced by AC systems. Hence, Asynchronous, Synchronous, Brushless Direct Current (BLDC) Motor and Switched Reluctance Motors started to be used in EVs. The demand for high performance electrical machines increases with increasing interest in EVs. Therefore, electrical machine designers have started to push the limits together with demands for high uninterrupted and maximum torque intensity, high efficiency and wide constant power interval and their improvement. For this purpose, various electrical machinery types emerged such as interior permanent magnet, surface permanent magnet, flux-switching and permanent magnet supported synchronous reluctance machines (Li *et al*. 2018).

High efficiency is desired where high torque at low speeds, wide constant power interval and low torque are required for electrical motors designed for use in EVs. Moreover, additional requirements have emerged such as reducing the increasing iron losses resulting from high magnetic flux density at high speeds. Hence, variable smart motors (Ogawa *et al*. 2017) or motors with variable parameters (Fukami *et al*. 2017) have been designed. Temperature is an important parameter since these motors include magnets. Power increase at a ratio of 43 % can be attained in these motors by applying isolation method at high temperatures (Raminosoa *et al*. 2017).

The emphasis was on BLDC motor design and prototype production due to various advantages such as high efficiency, silent operation, brushless and collector-free structure, the fact that they do not generate any electrical arc, ease of removing winding temperature, the ability to minimize electrical losses, the ability to generate high torque subject to stator diameter, higher yield and power/volume ratio in comparison with other low power motors. BLDC motor structure and operation, mathematical model and motor design calculations, modelling via Finite Elements Method (FEM) and motor analyses have been presented in detail. In addition, the study also includes the prototype manufactured for the designed model and its experimental verification.

The presented study consists of 5 sections. The first section is the Introduction. The second section provides an overview of BLDC motor. The third section includes analytical design and FEM analyses. The experimental setup installation and interpretation of the acquired experimental data are presented in section four. The final section includes all the results.

2. Materials ve Method

The performance of EVs is directly related with the performance of the electric motor used. The torque-speed or power-speed characteristics of the electric motor used have an impact on the performance of EVs (Xue *et al*. 2008, Grunditz and Jansson 2009). Thus, the selection of the motor to be used is very important for an EV.

It is possible to come across different motor types in EVs. These motors can be classified in different categories. One of these classifications is based on whether the motor is brushed or not. Various issues such as loss of efficiency due to brush and collector setup, usage difficulties and faults can be encountered in motors with brush and collector group.

The current state of magnet technology enables the motors with magnets to reach superior levels in comparison with other motors. BLDCs are preferred in many fields due to their advantages such as problem-free structure, high torque/current and

torque/inertia ratios, higher yield per unit volume and reliability (Yılmaz 2004).

BLDC motor structure develops by way of the reversal of permanent magnet synchronous motors from the inside towards the outside. BLDC is a synchronous motor type with three phase windings in its stator and a trapezoidal reverse electromagnetic force (Aydoğdu 2011). In BLDC motors that can be designed as single phase and three phase, the number of poles must be at least two. The number of poles can be designed in any number provided that it is an even number (Krause *et al*. 2002).

BLDCs have various advantages over other motors due to their silent operation, high efficiency, simple and low cost maintenance operations, their ability to operate in explosive environments without causing any hazardous incident, higher efficiency and power/volume ratios even at low power values and their ability to easily transfer winding temperatures to the external environment (Aydoğdu 2011). Hence, the BLDC motors are widely used in electric vehicles, medical fields, space crafts, and industrial automation systems (Çelikel 2019). Whereas the disadvantages of these motors are the requirement for different algorithms for starting and control, the need for instantaneous rotor position data for control, weakening and even complete disappearance of magnetic characteristics over time or based on use (Skvarenina 2002).

BLDCs can be classified in different ways and one of these classifications is based on the stator and rotor positions. They are known as inner-rotor if the stator covers the rotor and outer-rotor if the rotor encompasses the stator. Moreover, they are also classified as trapezoidal (square wave) and sinusoidal (sine wave) drive according to the type of reverse electromagnetic force in the windings. BLDCs have a wide range of application areas since they have different magnet levels, fixed coils and rotating magnets (Ying and Ertuğrul 1999).

Issues related with imbalance in rotor may develop in outer-rotor structure. Vibrations related with the impact of inertia can be indicated as one of these issues. Such motors preserve the constant value for speed during sudden changes in load arising from high inertia. Therefore, they have been frequently used in fan and washing machine applications (Kim 2003). The use of outer-rotor in BLDC provides various advantages such as; high inertia and less cogging torque impact, increase in output torque, torque change, high performance in low speed applications, silent operation (Hanselman 1994).

2.1 Selection of Motor Input Parameters

The characteristics of the vehicle that the motor will be applied on are among the primary parameters that need to be selected during the starting phase of the motor design process. ElektroGOP electrical racing vehicle has been taken as the reference in this study for the application. The dimensions of the vehicle are presented in Fig 1 and Table.1 (Akın 2019).

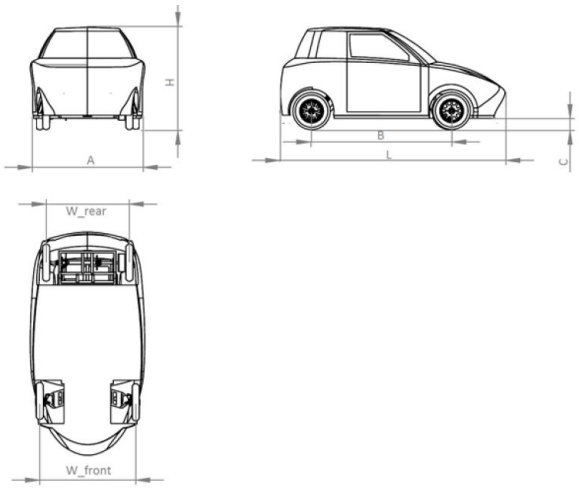

Figure 1. Sizing of the vehicle

Table 1. Vehicle dimensions

	Minimum (cm)	Value (cm)	Maximum (cm)
A	120	124	180
B	130	158	-
C	10	10	-
H	100	118	-
L	200	259	425
W_Front	100	107	-
W_Rear	80	106.5	-

The average weight of the designed vehicle including the driver (55 ~ 60 kg) is around 260 kg. The vehicle is expected to take 30 laps at a speed of 60 km/h on a track where the slope is approximately

0 degrees. Motor power calculated according to these parameters is approximately 1.5 kW. The electrical equipment of the vehicle was determined according to this value.

3. BLDC Motor Analytical and Electromagnetic Design

There are many studies and software for the sizing design of electrical machines. Traditional outer-rotor BLDC motor structure equations have been used for the motor design used in the present study (Boldea and Nasar 2002).

3.1 Calculation of the Motor Parameters for the Vehicle

The required shaft power was determined as 1.5 kW as a result of the calculations made using parameters such as vehicle mass, diameter of the tires of the vehicle, front surface area of the vehicle subject to the wind, friction coefficients of the tires, aerodynamic coefficient, air density, vehicle speed and gravity etc. Motor efficiency was obtained as η ~ %86. From here, the input power of the motor P_{in} was determined as;

$$\%\eta = \frac{P_{out}}{P_{in}} \quad (1)$$

The value of 1.74 kW is obtained using Equation (1). The rpm of the motor n is calculated using Equation (2).

$$n = \frac{120*f}{2p} \quad (2)$$

Here, f denotes the operating frequency and 2p represents the number of poles. The number of poles is taken as 46 and the rpm as 680 and when they are placed in the equation, the operating frequency is obtained as 260.67 Hz.

Rated torque (M_N) is the value obtained from the motor shaft operating at the rated frequency and rated rpm. It is calculated via Equation (3).

$$M_N = 9550 * \frac{Rated\ power\ (kw)}{Rotor\ rated\ speed\ (rpm)}\ (Nm) \quad (3)$$

The rated torque value is obtained from Equation (3) as 21.07 Nm.

Table 2 presents the values obtained by calculations based on the approximate average values of a 1.5 kW BLDC motor.

3.2 FEM Design

ANSYS RMxprt and ANSYS Maxwell software were used for the FEM based analyses of the designed motor. ANSOFT Maxwell software was used in the present study for carrying out analytical analyses via RMxprt after which FEM analyses were carried out via Maxwell 2D for the acquired analytical data. The flow diagram for the study is presented in Fig 2.

Figure 2. Motor design flow diagram

The designed motor has 46 poles and 51 slots. Fig 3 also shows the ANSYS Maxwell 2D geometry.

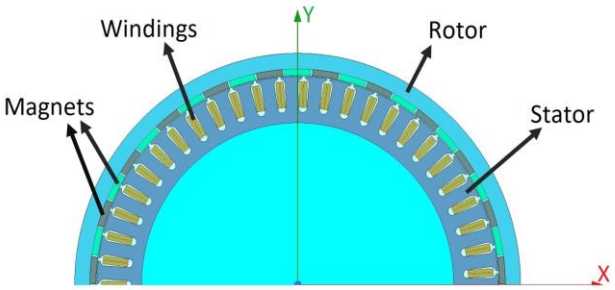

Figure 3. BLDC geometry

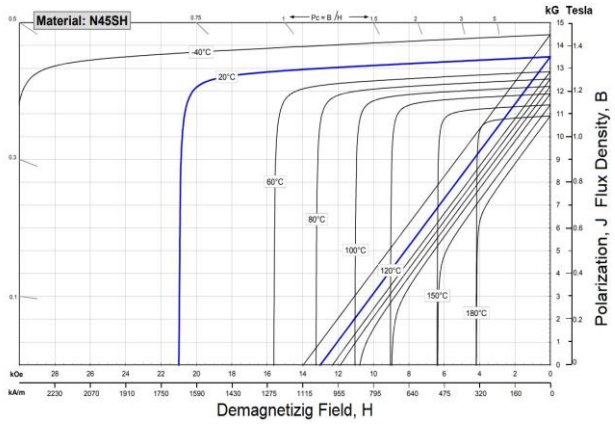

Figure 4. BH curve of the N45SH magnet

Table 2. Motor design parameters

Design parameters	Motor properties
Shaft Power	1.5 kW
Shaft speed	680 rpm
Battery voltage	48 V
Efficiency	~ %86
Number of poles	46
Operating frequency	50-300 Hz
Rated moment	21.07 Nm
Rotor material	ST37 Steel
Stator inner diameter	154 mm
Rotor outer diameter	220 mm
Motor stack length	40 mm
Working type	Direct Drive
Magnet strength temperature	150 °C
Magnet type	N45SH

Fig 4 shows the BH curve of the N45SH magnet used in motor design. In ideal permanent magnets, the BH curve is expected to be close to rectangular and fat. Thus, it is ensured that the area provided by the hysteresis curve is very large. Furthermore, considering the operating conditions of the BLDC motor, the temperature parameter is also an important factor in the selection of the magnet. The flux values of the N45SH type magnets are around 1.2 T at the operating temperatures of the vehicles. In addition, N45SH magnets begin to demagnetize after 150^{0}C temperature value.

3.3 Electromagnetic Analysis Results

Parametric resolutions were used for ensuring that the efficiency and other output parameters remain at the desired levels at the end of all sizing and optimization works via ANSOFT Maxwell as a result of which the 1.5 kW motor model took on its final form. Fig 5 shows the graph for the change in motor current obtained subject to the change in motor speed.

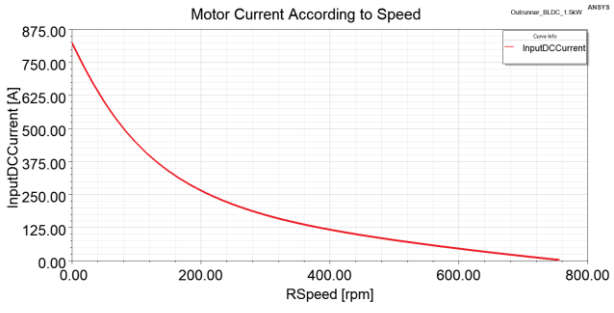

Figure 5. Change in motor current (A) subject to motor speed (rpm)

FEM analyses were carried out using the BLDC Maxwell RMxprt software examining parameters such as motor current, efficiency, shaft power, shaft torque, speed. The FEM results obtained put forth that motor current decreased subject to motor speed while motor efficiency increased up to the speed value of 680 rpm and decreased again after this value. Motor efficiency was maximum in the speed interval of 580 – 680 rpm. Even though the current parameter reaches values of up to 4.7 kW, it is not suitable to operate the motor in this region. Efficiency was determined as 87% at motor power value of 1.5 kW while torque was 22.56 Nm and speed was 635.87 rpm.

Transfer operation was carried out between Maxwell RMxprt and Maxwell 2D software after completing the FEM analyses for BLDC. The FEM analyses carried out are based on dividing the material into small node elements. The proximity of the results obtained via FEM analyses to actual results is proportional to the number of nodes. While the number of nodes is directly proportional with solution sensitivity, greater number of nodes speeds up the solution processes. Fig 6 presents the appearance of the model divided into nodes. A total of 73230 nodes were formed in the analyzed model with 9292 for the rotor, 42252 for the stator, 816 for the windings and 7744 for the magnets including those for the other parameters as well.

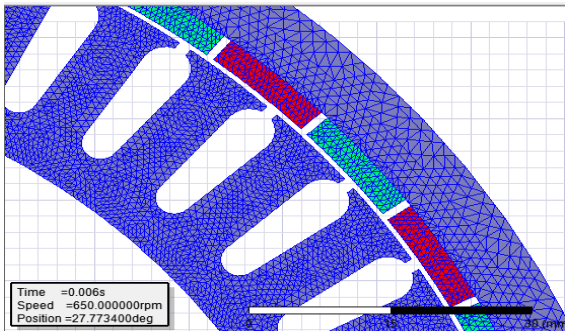

Figure 6. Appearance of the mesh process

Magnetic flux density is one of the parameters with an impact on motor performance. This value should be taken into consideration during motor design. Magnetic saturations in the material lead to loss of power in the motor which in turn affects efficiency. Magnetic flux density differs subject to the

properties of the material. Fig 7 shows the magnetic flux distribution for the designed motor.

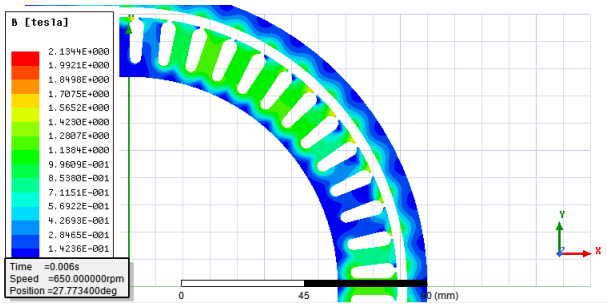

Figure 7. Magnetic flux density distribution

It can be observed when Fig 7 is examined that the flux distribution in the materials has taken place homogeneously. While the maximum flux value in the materials is 2.13 T, average flux density was obtained around 1.2 T.

Matlab software was used for comparing the values of shaft power, torque, and efficiency obtained for different magnet thicknesses the results of which are presented in the figures below.

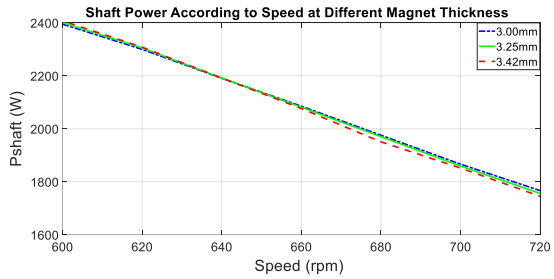

Figure 8. Speed – shaft power graph

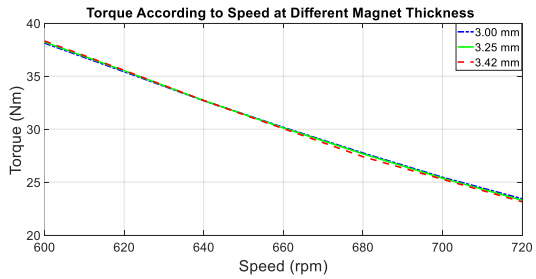

Figure 9. Speed – torque graph

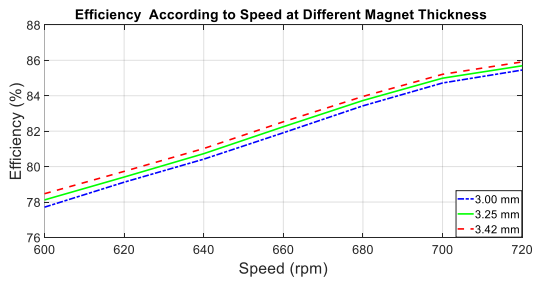

Figure 10. Speed – efficiency graph

Fig 8- Fig 10 show the graphs for shaft power, torque and efficiency respectively subject to change in revolution. It was observed when Fig 8 was examined that Pshaft value is greater than 2200W for 3 magnet thickness values when motor rpm was 600. It was observed upon examining the graph that motor shaft power decreases with increasing rpm. Shaft power was observed to be between 1600W-1800W for a rotor speed value of 700 rpm. Fig 9 shows that torque value decreases with increasing rpm. The maximum torque value obtained was 33 Nm. whereas it was observed that torque varied between 22-24 Nm motor in cases when motor rpm is 700. It was observed in Fig 10 that efficiency varies between 85% – 86 % when motor speed was about 700 rpm. While magnet thickness does not cause a significant difference in shaft power and torque graphs subject to rpm, it was observed in the efficiency graph that efficiency increased with increasing magnet thickness.

3.4 Thermal Results

Motor temperature is very important for motors with magnets. An increase in motor temperature results in deteriorations in the magnet structure. This leads to a decrease in the flux generated by the magnets and consequently reduced motor efficiency. Thermal analyses were carried out after completing the necessary definitions for the prototype motor following the FEM for 1.5 kW BLDC. Temperature values obtained with the motor operated for 120 minutes for thermal analysis; magnet temperature is 105 ° C. 45SH type magnet has been used in the prototype motor and the demagnetization temperature for this magnet is 150°C. Other temperature values for different motor parts were obtained as 113°C for stator windings, 112°C for stator yoke, 113°C for tooth, 104°C for rotor core and 95.5°C for the shaft. These values are in the boundary values for the materials used and it has been concluded that the selected design will not cause any thermal issues.

3.5 Cogging torque

Cogging torque is the torque that develops subject to the interaction of the stator slots and the magnets in the rotor in permanent magnet motors. While this torque does not have any impact on the load, it causes fluctuations in speed and vibration. This torque value depends on position and the number of stator slots. Required precautions should be taken for reducing cogging torque taking into consideration its impact on efficiency. Different slot gaps, auxiliary slots or shifting of the slot gaps may be taken as precautions for reducing this value while magnet or poles are shifted in the rotor or magnet steps are changed.

The 3 dimensional design of the motor was made for an accurate determination of cogging torque. The image for this design is presented in Fig 11. Analyses were made for the cogging torque calculated for each angular position of the rotor using the FEM model generated. Fig 12 shows the graph for cogging torque. It can be observed from the graph that the peak values for cogging torque are in the 0.2 Nm interval. It was concluded based on these values and the FEM analyses for the prototype motor that cogging torque values are not problem for motor manufacturing.

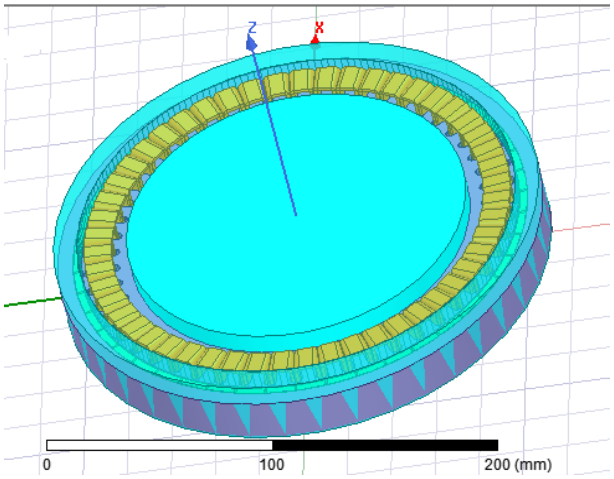

Figure 11. Motor 3D model

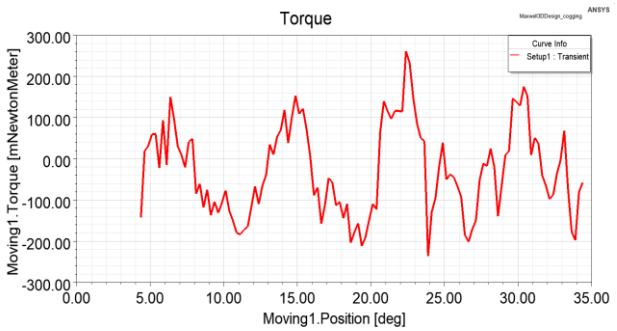

Figure 12. Cogging torque graph

3.5 BLDC motor prototype manufacturing and experiment setup

Motor manufacturing (mechanical labor) is very important for the experimental verification of the results obtained by way of analytical design and FEM. Hence, prototype manufacturing is one of the most difficult steps. Any mistake or shortcomings in mechanical processes during prototype manufacturing lead to disadvantages in the motor.

The best result was obtained as a result of the analytical calculations and prototype manufacturing was carried out based on traditional BLDC motor methods with a slot / pole ratio of 51 / 46. Traditional packaging method from siliceous sheet metal for the stator of the prototype motor, while Steel 1010 was processed on the turning lathe during rotor manufacturing thus taking on its final shape. The manufactured magnets were affixed to the rotor via adhesives with high viscosity. Fig 13 shows various pictures from manufacturing.

Figure 13. Production photographs (a- rotor, b- frame, c-wound stator, d-integrated to the wheel)

3.6 Experimental setup for the BLDC

The test setup in Fig 14 was prepared for determining the BLDC motor performance. The DC motor was used with a square body and a shaft power of 10 kW coupled to the shaft of the BLDC motor in the same axis. A 1024 ppr incremental coding encoder was used for speed data, while a load cell was used for torque measurement. Motor current and voltage, motor speed, load torque, motor shaft power and input power can be recorded with the test setup.

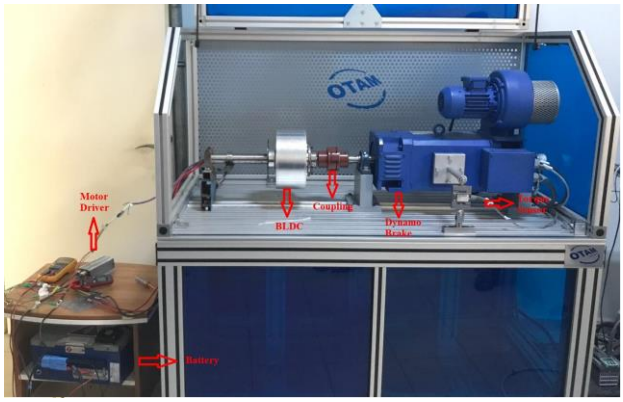

Figure 14. Test setup

4. Experimental Results and Discussion

4.1 *Performance experiments*

Test scenarios were prepared for measuring the efficiency, speed, torque, current and power curves of the motor.

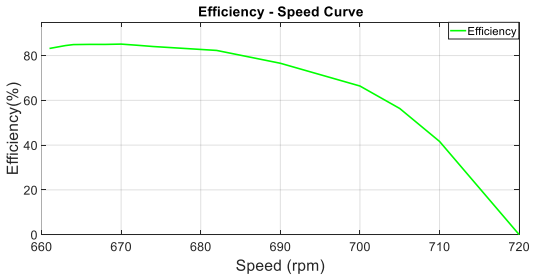

Figure 15. Motor speed – efficiency curve

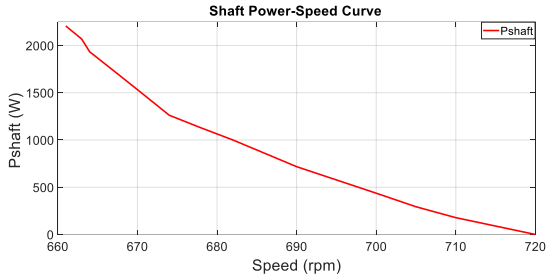

Figure 16. Motor speed –shaft power curve

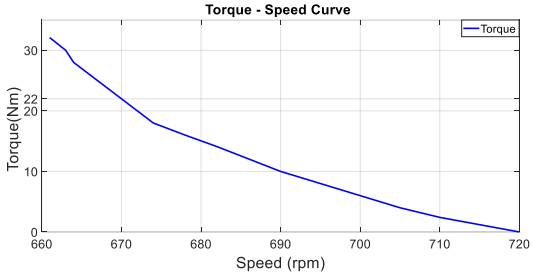

Figure 17. Motor speed – torque curve

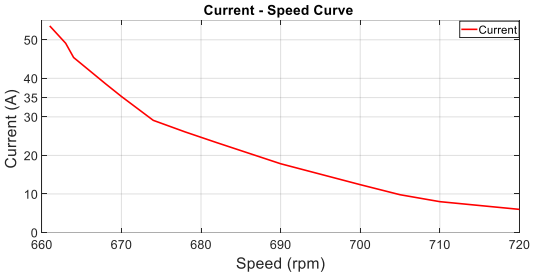

Figure 18. Motor speed – current curve

It was observed when Fig 15 - Fig 18 were examined that the results obtained are close to the power (1.5 kW) and speed value (680 rpm) targeted during the design process. Whereas motor efficiency was obtained as about 85% at these values. The current drawn by the motor when rotating at a speed of 670 rpm was obtained as 35 A and the torque value was 22 Nm. When FEM results and experimental results are compared, it is seen that there are deviations of approximately 30 rpm in speed and 100W in power for the same torque value. In this situation, the differences arising from the production of the model designed with FEM can be shown. In addition, it is thought that the sensitivity of the experimental setup has also affected. However, these deviation values are in the acceptable range.

4.2 *Heating experiment*

Nominal power is defined during the calculations for motor design as the maximum power that can be provided by the motor under normal conditions. The temperature of the motor parts starts to increase when the motors are operated under excessive load. This increase may lead to undesired instances such as deterioration of the motor windings or the magnets losing their characteristics. The motor was operated at full speed for about 30 minutes prior to carrying out the data acquisition procedure during the experimental study and the winding temperature at ambient temperature (about 25°C) was increased up to 65°C. Afterwards, maximum winding temperature was measured as 108°C as a result of the 30 minute experiment carried out for obtaining the performance curves. A 5 °C difference was observed with the FEM heating results. This difference can be indicated to be due to the assumptions made during motor design and motor casing ventilation. It was observed based on the simulation and experiment results that the thermal load of the motor has remained between the boundary values with regard to winding isolation and the safe operating temperature for the magnets.

4.3 Integration of the Motor to the Vehicle

The motor was mounted on a 10 inch rim for integration to the vehicle of the prototype motor that yields the desired simulation and experimental results. The motor was mounted on the vehicle using a pillow block. The brake disk, brake damper and hydraulic hoses were connected thus making it ready for road tests. It was observed during the test drives that the desired torque and speed values have been attained and that the motor operates without any problem. Fig 19 shows the prototype motor mounted on the vehicle.

Figure 19. Mounting of the motor to the vehicle

5. Conclusions

In this study, design parameters based on the physical, magnetic and thermal needs of the motor were determined for the 48 V, 680 rpm BLDC motor prototype which was designed and manufactured. The first sample design emerged after deciding on values such as motor dimensions, torque, power and speed in addition to selecting the number of slots/poles and the winding model along with the constant values.

To reach to optimum model, several parameters pre-determined during the design stage such as the number of windings, magnet type and magnet thickness were varied in order to examine the analyses and continue the optimization process after which the impacts of the differences were examined. Integration between the motor driver and the motor was established and the experiment setup was prepared in order to carry out the experiments on the designed and manufactured motor with a shaft power of 1.5 kW and with 51 slots/46 poles. The aim of the experiments was to determine how close the operating values of the motor are to the design values. Results obtained during the analytical, simulation and experimental studies on the motor were presented comparatively after these studies. Finally, the motor was integrated to the vehicle with a 10 inch rim and it was concluded that it operates between the targeted values.

6. References

Akın, F., 2019. Electric vehicles developed for external-rotor brushless dc motor design and analysis. M.Sc. Thesis, Tokat Gaziosmanpasa University Graduate School of Natural And Applied Sciences, Tokat, 84.

Aydoğdu, Ö., 2011. An effective real coded GA based fuzzy controller for speed control of a BLDC motor without speed sensor. *Turkish Journal of Electrical Engineering and Computer Sciences,* **19 (3)**, 413-430.

Boldea, İ. and Nasar, S.A., 2002. The induction machines desing handbook - Second edition. *Taylor and Francis Group*, United States of America, 490-640.

Fukami, T., Motoki, K., Kirihata, R., Shima, K., Koyama, M., Mori, T. and Nakano, M., 2017. An electromagnet-assisted ferrite magnet motor, *IEEE Transactions on Magnetics*, **53 (11)**, 1-4.

Çelikel, R., and Aydoğmuş, Ö., 2019. A torque ripple minimization method for brushless dc motor in high speed applications. *Journal of Engineering Research*, **7** (3), 200-214.

Gökce, C., 2005. Modeling and simulation of a series parallel hybrid electrical vehicle. Istanbul Technical Unıversity, Institute of Science and Technology, İstanbul, 64.

Grunditz, E. and Jansson, E., 2009. Modelling and simulation of a hybrid electric vehicle for shell ecomarathon and an electric gokart, M.Sc. Thesis, Chalmers University of Technology Electric Power Engineering, Göteborg, 10-12.

Hanselman, D.C, 1994. Brushless permanent-magnet motor design. I, Mc Graw- Hill, ABD, 61-101.

Hori, Y., 2004. Future vehicle driven by electricity and control-research on four-wheel- motored, *IEEE Transactions on Industrial Electronics*, **51 (5)**, 1-14.

Kim, S., Choi, J. and Lee, J., 2003**.** Magnet shape optimization for high performance single-phase line start synchronous motor. *Journal of Applied Physics*, **93 (10)**, 8695-8697

Krause, P., Wasynczuk, O. and Sudhoff, S.D., 2002. Analysis of electrıc machinery and drive systems. 2nd ed., IEEE Press, USA, 67-106.

Li, Y., Bobba, D., and Sarlioglu, B., 2018**.** Design and optimization of a novel dual-rotor hybrid pm machine for traction application. *IEEE Transactions on Industrial Electronics*, **65 (2)**, 1762-1771.

Ogawa, T., Takahashi, T., Takemoto, M., Ogasawara, S., and Daikoku, A., 2017. The examination of pole geometry of consequent pole type ferrite PM axial gap motor with field winding. *In Electric Machines and Drives Conference (IEMDC)*, 2017 IEEE International, pp. 1-7.

Raminosoa, T., El-Refaie, A. M., Torrey, D. A., Grace, K., Pan, D., Grubic, S., and Huh, K. K. 2017. Test results for a high temperature non- permanent-magnet traction motor. *IEEE Transactions on Industry Applications*, **53 (4)**, 3496-3504.

Skvarenina, T. L., 2002. The power electronic handbook. I, CRC Press LLC, New York, 78-100.

Tur, O., Tuncay, R.N. and Ucarol, H., 2005. Basics of electric vehicle technology and a design study on a series hybrid electric vehicle powertrain. *ELECO 2005 4th International Conference on Electrical and Electronics Engineering*, Bursa.

Tur, O., Uçarol, H., Özsu, E., Demirci, M., Solak, Y., Elcik, E., Dalkılıç, Ö. and Özatay, E., 2007. Sizing, design and prototyping of an electric drive system for a split drive hybrid electric vehicle, International Electric Machines and Drives Conference (IEMDC) 2007, Antalya.

Tutelea, L. and I. Boldea, I., 2007. Optimal design of residential brushless d.c. permanent magnet motors with FEM validation, *Aegean Conference on Electric Machines*, Power Electronics and Electromotion (ACEMP'07), 435-439.

Ustun, O., Yilmaz, M., Gokce, C., Karakaya, U. and Tuncay, R., 2009. Energy Management Method for Solar Race Car Design and Application, *IEEE International Electric Machines and Drives Conference*, 804-811.

Uçarol, H., 2003, Hybrid electric vehicle, M.Sc. Thesis, Istanbul Technical Unıversity, Institute of Science and Technology, İstanbul, 89.

Xue, X. D., Cheng, K.W.E. and Cheung, N.C., 2008**.** Selection Of Electric Motor Drives For Electric Vehicles, *Australasian Universities Power Engineering Conference*, Hong Kong, 170-175.

Yılmaz, M., Tuncay, R.N. and Ustub, O, 2004. A wavelet study of sensorless control of brushless DC motor through rapid prototyping approach, *Proceedings of the IEEE International Conference on Mechatronics, ICM '04,* İstanbul, Turkey.

Ying, L. and Ertugrul, N., 1999. The Dynamic Simulation of the Three-Phase Brushless Permanent Magnet AC Motor Drives with LabVIEW, *Australasian*

Universities Power Engineering Conference AUPEC'99, Darwin, 11-16.

Zarko, D., Ban, D. and Lipo, T.A., 2007. Analytical Solution for Cogging Torque in Surface Permanent-Magnet Motors Using Conformal Mapping, I*EEE Transactions on Magnetics*, **44 (1)**, 52-64